Title: Effects of vegetation on bacterial communities, carbon and nitrogen in dryland soil surfaces: implications for shrub encroachment in the southwest Kalahari

Author names: Shubin Lan[a,b,*], Andrew D. Thomas[a], Stephen Tooth[a], Li Wu[a,c], David R. Elliott[d]

[a] Earth Surface Processes Research Group, Department of Geography and Earth Sciences, Aberystwyth University, Aberystwyth, SY23 3DB, UK

[b] Key Laboratory of Algal Biology, Institute of Hydrobiology, Chinese Academy of Sciences, Wuhan, 430072, China

[c] School of Resources and Environmental Engineering, Wuhan University of Technology, Wuhan, 430072, China

[d] Environmental Sustainability Research Centre, University of Derby, Derby, UK

* Tel/Fax.: +44 (0)1970 622580; E-mail address: shl25@aber.ac.uk

Abstract

Shrub encroachment is occurring in many of the world's drylands, but its impacts on ecosystem structure and function are still poorly understood. In particular, it remains unclear how shrub encroachment affects dryland soil surfaces, including biological soil crust (biocrust) communities. In this study, soil surfaces (0-1 cm depth) were sampled from areas of *Grewia flava* shrubs and *Eragrostis lehmanniana* and *Schmidtia kalahariensis* grasses in the southwest Kalahari during two different seasons (March and November). Our hypothesis is that the presence of different vegetation cover types (shrubs versus grasses) alters the microbial composition of soil surfaces owing to their contrasting microenvironments. The results showed that more significant differences in microclimate (light, soil surface temperatures) and soil surface microbial communities were observed between shrubs and grasses than between sampling seasons. Based on high-throughput 16S rRNA gene sequencing, our findings showed that approximately one third (33.5%) of the operational taxonomic units (OTUs) occurred exclusively in soil surfaces beneath shrubs. Soil surfaces with biocrusts in grass areas were dominated by the cyanobacteria *Microcoleus steenstrupii*, whereas the soil surfaces beneath shrubs were dominated by the proteobacteria *Microvirga flocculans*. Soil surfaces beneath shrubs are associated with reduced cyanobacterial abundance but have higher total carbon and total nitrogen contents compared to biocrusts in grass areas. These findings infer changes in the relative contributions from different sources of carbon and nitrogen (e.g. cyanobacterial and non-cyanobacterial fixation, plant litter, animal activity). The distinctive microbial composition and higher carbon and nitrogen contents in soil surfaces beneath shrubs may provide a positive feedback mechanism promoting shrub encroachment, which helps to explain why the phenomenon is commonly observed to be irreversible.

Keywords: shrub encroachment; biocrusts; cyanobacteria; *Microcoleus*; carbon; nitrogen

Graphical Abstract

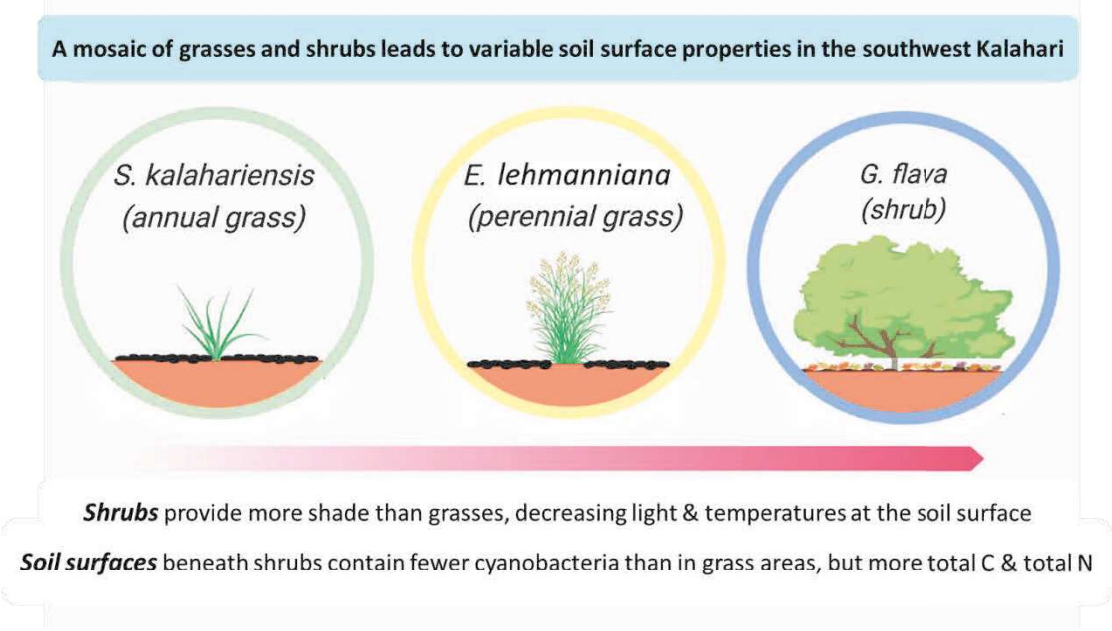

Highlights:

- Distinct soil surface bacterial communities occur in grass and shrub areas
- More operational taxonomic units occurred exclusively in soils beneath shrubs
- Soils beneath shrubs have lower cyanobacterial abundance but more total C and N
- Results infer that sources of C and N in grass and shrub areas are different
- Findings have implications for assessment and management of shrub encroachment

1. Introduction

Drylands is an umbrella term for the hyperarid, arid, semiarid and dry-subhumid environments that collectively cover more than 40% of the global land area (Adeel et al., 2005; Reynolds et al., 2007). In many of the world's drylands, a combination of climate changes and human activities are leading to negative impacts on ecological and landscape functions (Huang et al., 2016; Maestre et al., 2016; Berdugo et al., 2020), in some cases leading to dryland degradation. A commonly reported but contested process of dryland degradation is shrub encroachment (Eldridge et al., 2012; Stevens et al., 2017), which is defined as the increase in coverage, density and biomass of woody plants (Van Auken, 2009). Several models and theories have been developed to describe the processes of shrub encroachment, and collectively outline a variety of possible causal mechanisms including overgrazing, increases in global atmospheric CO_2 concentrations, and changes in fire frequency and intensity (Sankaran et al., 2005; Leakey et al., 2009; Belayneh and Tessema, 2017). The broader ecological consequences of shrub encroachment are complex and involve changes in soil and microclimate characteristics (Maestre et al., 2009; Eldridge et al., 2011; Belayneh and Tessema, 2017; Thomas et al., 2018). There may be additional, but as yet poorly documented, complexity affecting soil surfaces and biological soil crusts (hereafter called biocrusts), due to changes in the composition of the microbial community (Eldridge et al., 2011; Hu et al., 2012; Belnap et al., 2016; Belayneh and Tessema, 2017).

Biocrusts form at the interface between the atmosphere and soil through microbial colonisation of the soil surface by photoautotrophic cyanobacteria, microalgae, lichens, and mosses, as well as heterotrophic bacteria and microfungi. Although ubiquitous in drylands, biocrust composition varies spatially and with developmental status (Elliott et al., 2014; Belnap et al., 2016; Swenson et al., 2018).

As a pioneer colonising species, cyanobacteria play important roles in biocrust formation and development, and are a widely reported constituent of biocrusts either directly on the surface or within the uppermost few millimetres (Hu and Liu, 2003; Lan et al., 2012). As biocrusts develop, however, other photoautotrophic and heterotrophic organisms can become dominant, including lichens, mosses and bacteria such as firmicutes (Maier et al., 2018; Swenson et al., 2018), which reduces the relative importance of cyanobacteria. Regardless of their composition, biocrusts play an important role in stabilizing soil surfaces and increasing soil fertility in drylands (Belnap and Gillette, 1997; Elbert et al., 2012; Yan-Gui et al., 2013; Elliott et al., 2019) and can also regulate the local water cycle, affect seed germination and vascular plant growth, and provide habitats for small animals (Zhang et al., 2006; Li et al., 2011; Zhao et al., 2014).

In dryland ecosystems, biocrusts are typically distributed in the gaps between vascular plants (hereafter, vegetation), forming a landscape mosaic of macroscopic vegetation patches and biocrust patches (Li et al., 2010). As a result, carbon and nitrogen originating from biocrust organisms provide an additional source to the soil distinct to that originating from vegetation. Biocrust development further changes the soil microclimate, which affects germination, growth and productivity of vegetation (Lan et al., 2014a; Thiet et al., 2014). Many studies conclude that biocrusts do not compete with vegetation and that the colonisation of the spaces in between plants by biocrusts is an efficient use of limited dryland resources (Li et al., 2010; Belnap et al., 2016). Vegetation can limit soil surface ventilation and light incidence, however, thereby restricting the growth and development of biocrusts (Martínez et al., 2006; Briggs and Morgan, 2008). Although it is well established that vegetation strongly influences the microbial composition of soil in the rhizosphere (e.g. Dotaniya and Meena, 2015), the effect of vegetation on soil surface microbial communities is less well known. The relationship between biocrusts

and vegetation is thus complex and dynamic (Zhang et al., 2013; Bowker et al., 2016).

Our hypothesis is that the presence of different vegetation cover types (shrubs and grasses) in the southwest Kalahari alters the microbial composition of the soil surface. This hypothesis is important to test because a change in microbial composition of the soil surface is likely to constitute a functional change in the ecosystem. In particular, cyanobacteria play vital roles in biocrust formation and development, but there is only limited understanding of how these autotropic communities are affected by changes in vegetation cover. This study is a new analysis of soil surface and biocrust microbial communities from the southwest Kalahari, using data originally published by Elliott et al. (2014). Elliott et al. (2014) demonstrated clear bacterial community heterogeneity and niche partitioning in biocrusts and subsoils across different vegetation cover types (trees, shrubs, grasses), but they did not investigate the taxonomic details of the cyanobacterial communities. In the present study, the high-throughput sequencing data from Elliott et al. (2014) have been re-analysed to precisely identify the taxonomic assignment of the dominant bacteria and particularly all the cyanobacterial species, and the results are combined with new analyses of the carbon and nitrogen content associated with soil surfaces from shrub and grass areas. These new analyses enable us to address the following research questions: 1) how does the presence of shrubs and grasses affect the microbial composition, diversity and cyanobacterial abundance in dryland soil surfaces?; and 2) how do differences in vegetation cover type and soil surface microbial community compositions affect total carbon and total nitrogen? The answers to these questions provide insights into the dominant sources of carbon and nitrogen and may have important implications for assessing and managing shrub encroachment in the southwest Kalahari, and potentially in other drylands worldwide.

2. Methods and materials

2.1 Study location

The study location is on rangeland that is 980 m above sea level and 10 km northeast of Tsabong in the Kgalagadi District of Botswana (25˚ 56’ 51’’ S, 22˚ 25’ 40’’ E - Fig. 1A). Mean annual precipitation is ~300 mm and annual potential evapotranspiration exceeds 2000 mm (UNESCO, 2016). The area is characterized by vegetated, stabilized, linear dunes. Soils are fine-grained sandy, weakly acidic (pH 5.8 ± 0.2) arenosols (Food and Agriculture Organisation, 2015), typically with low carbon (0.55 ± 0.03%) and low nitrogen (0.04 ± 0 .01%) concentrations, and with little or no horizon development (Wang et al., 2009; Thomas, 2012; Fig. 1B). Vegetation is a mix of trees (*Vachellia* spp.*)*, shrubs (*Grewia flava* and *Senegalia mellifera*), and perennial and annual grasses, mainly *Eragrostis lehmanniana and Schmidtia kalahariensis* respectively (Elliott et al., 2014; Thomas et al., 2018; Fig. 1C-E). The land is used for cattle, goat and sheep grazing, which typically leads to reductions in biocrust and perennial grass cover (Thomas and Dougill, 2007), and when grazing is prolonged and intense, to a reduction in the ability of biocrusts to sequester and store carbon (Thomas, 2012).

2.2 Sample collection

Field sampling and data collection was undertaken in November 2011 at the end of the winter dry season and in March 2012 toward the end of the summer wet season. From July 2011 to June 2012 the mean air temperature was 23.8 ºC and there were 3661.5 hours of sunshine (Fig. S1). Mean air temperatures were similar in November (28.0 ºC) and March (29.0 ºC). Total precipitation from July 2011 to June 2012 was 281.7 mm, occurring over 55 rain days, with >80% of the total falling between

December and March (Fig. S1).

To reduce the potential impact of recent grazing, domesticated animals had been excluded from the study location for one year before sampling. At the time of sampling, biocrusts covered about 30% of the soil surface (Elliott et al., 2014; Fig. 1B). For the purposes of this study we use the term 'biocrust' to describe all samples collected from grass areas, which have previously been shown to contain high levels of cyanobacteria in the soil surface (Elliott et al., 2014). In contrast, the shrub-dominated areas had lower levels of cyanobacteria in the soil surface. Therefore, by some definitions soil surface samples from shrub areas may not be regarded as biocrusts *sensu strictu*, so we avoid that term even though in all cases the uppermost ~0.5 cm of the soil was biologically consolidated into a crust. In November and March, the uppermost 1 cm of soil, which included biocrusts where present, was collected aseptically using sterile spatulas from *E. lehmanniana* and *S. kalahariensis* grass interspaces and from beneath *G. flava* shrubs (Table 1). In both seasons, samples were collected from three sites associated with each vegetation type (3 x annual grasses, 3 x perennial grasses, 3 x shrubs), with each site separated by a minimum of 20 m (Elliott et al., 2014). All samples were dry at the time of sampling, but additional air drying was carried out as a precaution to ensure dry storage prior to carbon and nitrogen determination. DNA was extracted from samples within 18 hours of collection (details in Elliott et al., 2014).

2.3 Total carbon and nitrogen content and vegetation microclimate

Total carbon and total nitrogen contents of the samples (including biocrusts and any attached soil) were determined using a TruSpec elemental analyser (Leco Corp., USA; Elliott et al., 2014). Solar radiation in shrub and grass sites was measured continuously during each sampling season using

photosynthetically active radiation (PAR) sensors (Skye Instruments Ltd., UK), and the soil surface temperature and moisture content at each site were recorded simultaneously using temperature/moisture sensors (Decagon Devices Inc., USA).

2.4 Bacterial community annotation

DNA extraction and sequencing were undertaken for a previous study (Elliott et al., 2014), and the sequencing data in this study were downloaded directly from the MG-RAST database (http://metagenomics.anl.gov/linkin.cgi?project=6691). The raw sequences were then processed in Mothur (version v1.30.1) to remove barcodes, adaptors, primers, and ambiguous bases (Luo et al., 2013). The optimized sequences with average size of 560 bp were clustered into different OTUs at a similarity level of 97% using Usearch (version v7.1 http://drive5.com/uparse/; Edgar, 2013), and chimeric sequences were identified and removed using UCHIME (Edgar et al., 2011). Each OTU was given a sequence representative, and all the sequences of each OTU were aligned using the SILVA SSU rRNA database through RDP classifier (Release123 http://www.arb-silva.de) to obtain OTU taxonomic information at phylum level, including cyanobacteria and other bacterial phyla (Wang et al., 2007). Similarly, the taxonomic information at genus level of each OTU was obtained from the SILVA SSU rRNA database. Relative abundance of each OTU was defined as the percentage of OTU sequences in all the bacterial sequences. Good's coverage (the percentage of sequenced species in the community) and Shannon index were calculated using Mothur to indicate the depth of sequencing and bacterial diversity, respectively (Deng et al., 2014).

2.5 Dominant and cyanobacterial OTU phylogenetic identification

OTUs whose sequences accounted for more than 1% of the total sequences across all samples were defined as dominant OTUs (Urbanová et al., 2015). BLAST analysis of representative sequences of the dominant bacterial and all cyanobacterial OTUs was conducted to manually verify the RDP classifier taxonomy by examining closely related sequences from the GenBank database (Muñoz-Martín et al., 2019). The taxonomic placement of cyanobacterial OTU sequences was additionally checked using the Cydrasil software (version 1.5; Giraldo-Silva et al., 2020), which is a curated cyanobacterial database for 16S rRNA gene sequences, further described in Machado-de-Lima et al. (2019). In cases where the Cydrasil analysis gave a different result to the GenBank based taxonomy assignment, both results were used in the phylogenetic evolutionary analysis to assess which result had the closer genetic distance to our sequences. Those sequences with genetic distance ≤0.03 were considered to be the same species, and those with genetic distances >0.03 but ≤0.05 were considered to be different species of the same genus (Rossi-Tamisier et al., 2015).

2.6 Statistical and data analyses

Bacterial communities at phylum level were clustered with hierarchical clustering using MEV software (Howe et al., 2011). Nucleotide sequence phylogeny was analyzed with Maximum Likelihood Tree, and the genetic distance between sequences was calculated via the Pairwise Distance with the Maximum Composite Likelihood substitution model. The phylogenetic assignment and genetic distance were analyzed using Mega 6.0 software (Tamura et al., 2013). The difference of each variable (Shannon index, cyanobacterial abundance, photosynthetically active radiation (PAR), soil temperature, and total

carbon and total nitrogen contents) between the different vegetation cover types or different sampling seasons was analyzed by a non-parametric (Kruskal-Wallis) test using SPSS v. 20.0. To evaluate the relationships between cyanobacterial abundance (the percentage of cyanobacterial sequences in all the sequences) and total carbon and total nitrogen contents, cyanobacterial abundances were log(x+1) transformed, and then curve fitting was applied via Curve Estimation using SigmaPlot 12.5.

3. Results

3.1 Vegetation microclimate

At the time of sampling in November and March, it had not rained at the study location for at least 3 days and the soil surfaces contained very little moisture (<0.1% v/v). The shrub canopies created a shaded understorey, where photosynthetically active radiation was 13-37% of that at the less shaded grass sites (P <0.05; Fig. 2A-B; Table S1). During the two sampling seasons, there were no significant differences in soil surface temperatures (P = 0.824; Fig. 2C-D; Table S1). Soil surface temperatures were, however, significantly different between vegetation cover types (P < 0.05; Table S1; Fig. 2C-D).

3.2 Microbial community structures

Bacterial community composition, diversity and cyanobacterial abundance varied with vegetation cover type, but for each cover type, communities were similar in each season (Fig. 3; Tables S1 and S2). In total, 617 OTUs were obtained, and just over one-third of the OTUs (n = 211, 34.2%) were shared across the three cover types (Fig. 4). Up to 207 OTUs (33.5%) occurred exclusively in the soil surfaces beneath shrub cover, while only 20 OTUs (3.2%) and 48 OTUs (7.8%) were restricted to the biocrusts

171 in grass areas (*E. lehmanniana* and *S. kalahariensis*), respectively (Fig. 4A). Regardless of the sampling
172 season, the frequency of occurrence of OTUs could be well predicted by their relative abundance (P
173 <0.0001; Fig. 4), which suggests that there is a close relationship between the relative abundances of
174 OTUs and the associated vegetation type. Depending upon whether taxa were found in association with
175 all three cover types or were exclusive to shrub or grass areas, we tentatively defined them as generalists
176 or specialists, respectively.

177 In total, 224 taxa were classified to genus level, and 118 different genera were identified (Table
178 S2). *Microcoleus* species (phylum cyanobacteria) accounted for 27.0% of the sequence reads (relative
179 abundance) in grass areas (Fig. 5; Table S2) but less than 0.1% beneath shrubs. In contrast, *Microvirga*
180 species (phylum proteobacteria) were more abundant beneath shrubs (10.5%) compared to grass areas
181 (1.6%) (Fig. 5; Table S2).

182

183 ***3.3 Dominant and cyanobacterial OTUs***

184 The 12 dominant bacterial OTUs across all soil surface samples were distributed in 5 phyla, namely
185 acidobacteria, actinobacteria, chloroflexi, cyanobacteria and proteobacteria (Fig. 5). Together these 12
186 dominant OTUs accounted for 17.9% of sequences in soil surfaces beneath shrubs, and for 58.6% and
187 38.9% of sequences in biocrusts associated with *E. lehmanniana* (LG)) and *S. kalahariensis* (SG) grass
188 areas, respectively (Fig. 5). In grass areas, OTU292 dominated the biocrusts (26.5%) and was identified
189 as the cyanobacterium *Microcoleus steenstrupii*. In contrast, in soil surfaces beneath shrubs, OTU320
190 (7.6%) was dominant and identified as heterotrophic nitrogen-fixing *Microvirga flocculans* (formerly
191 classified as *Balneimonas flocculans*; Weon et al., 2010) (Fig. 5).

192 According to the phylogenetic assignment (Fig. 6), 10 cyanobacterial OTUs of 8 clades were
193 identified to species or genera level, whilst 6 OTUs had a genetic distance >0.05 with the identified
194 cyanobacterial species in Genbank or a bootstrap value <40%. The OTUs in clades 2, 3, 4, 5 and 6 fell
195 into their respective species/genera gathering representative sequences, in which OTU331, OTU579,
196 OTU537, OTU520 and OTU559 were identified as *Microcoleus steenstrupii*, *Crinalium* sp.,
197 *Chlorogloea* sp., *Scytonema hyalinum* and *Scytonema* sp., respectively (Fig. 6). Clades 1, 7 and 8,
198 however, included at least two genera with high similarity (>97%). In clade 1, OTU214 and OTU292
199 were identified as *Microcoleus steenstrupii* owing to their highest similarity to *Microcoleus steenstrupii*
200 187-2 (AJ871986). In clade 7, the cyanobacterial species belong to *Coleofasciculaceae*,
201 *Leptolyngbyaceae*, *Oscillatoriaceae*, and *Pseudanabaenaceae* (Komárek et al., 2014). All the retrieved
202 species had very high similarity with OTU179, so cannot be distinguished easily. Clade 8 included
203 species of *Crinalium* and *Starria*, in which OTU72 and OTU498 were identified as the genus *Crinalium*
204 owing to their high similarity to *C. epipsammum* SAG 22.89 (NR 112218 or AB115964).
205

206 ***3.4 Total carbon and total nitrogen***

207 The total carbon and total nitrogen content of the soil surface samples ranged from 1.82-9.64 g kg^{-1}
208 and 0.10-0.88 g kg^{-1}, respectively. Total carbon and total nitrogen concentrations were significantly
209 different between vegetation cover types (P <0.05; Fig. 7) but typically did not differ significantly
210 between sampling seasons (P >0.05; Table S1). Both total carbon and total nitrogen contents beneath
211 shrub cover were significantly higher than in grass areas (P <0.05; Fig. 7). Across all soil surface
212 samples, we found that there was a highly significant linear relationship between total carbon and total

213 nitrogen contents (y = 0. 011+0.080x; R^2 = 0.841; P <0.001; Fig. 8A), with the ratio of carbon to
214 nitrogen maintained at approximately 9.9:1. In contrast, there was a negative exponential relationship
215 between cyanobacterial abundance and total carbon content (R^2 = 0.543; P <0.001; Fig. 8B). Similarly,
216 cyanobacterial abundance decreases with increasing total nitrogen content (R^2 = 0.314; P = 0.009; Fig.
217 S2).
218

219 **4. Discussion**

220 In this study, we examined soil surface bacterial communities associated with different vegetation
221 cover types, with special attention given to the cyanobacterial taxonomy. The prior work of Elliott et al.
222 (2014) characterised the whole microbial community in biocrusts and subsoils. An important finding
223 was that cyanobacteria were substantially depleted in soil surfaces beneath shrubs, but the
224 cyanobacterial taxonomy and the biogeochemical implications of their depletion were not explored.
225 Therefore, in the present study, we conducted precise phylogenetic identification of the dominant
226 bacterial and all cyanobacterial species, and determined the total carbon and nitrogen content of soil
227 surfaces to establish whether there are any variations with vegetation cover. Our findings provide more
228 details on the effects of vegetation cover and associated understorey microclimates on soil surface
229 microbial communities, which may have functional implications for the southwest Kalahari ecosystem.
230 In particular, our data provide an insight into potential carbon and nitrogen sources, with implications
231 for a better understanding of shrub encroachment in the southwest Kalahari.
232

233 ***4.1 Vegetation microclimates and effects on soil surface bacterial communities***

234 During both sampling seasons, and for all of the vegetation cover types, soil moisture content was
235 very low (<0.1% v/v), and solar radiation and soil surface temperatures were very similar (P >0.05;
236 Table S1). These results likely explain the observed lack of difference in bacterial diversities and
237 cyanobacterial abundances between seasons. The highest solar radiation was recorded at the grass sites,
238 and this is where cyanobacteria were most abundant (34.5%; Fig. 3B). This finding may reflect the
239 ability of cyanobacteria to tolerate high levels of solar radiation (Garcia-Pichel and Pringault, 2001;
240 Lan et al., 2014b). The greater shading provided by shrub canopies and their litter layer might be an
241 important reason for the reduced cyanobacterial abundance beneath shrubs, as the reduced incident light
242 limits the potential for photosynthesis. Previously, Lan et al. (2015) demonstrated that cyanobacterial
243 metabolism and biomass accumulation decrease with decreasing light intensity, although some
244 cyanobacterial metabolic activities can be maintained temporarily by absorbing the secreted
245 exopolysaccharide as an alternative energy source (Mager and Thomas, 2011; Lan et al., 2015).
246 Species of the genus *Microcoleus* are commonly the dominant cyanobacteria in biocrusts, and
247 typically show regional biogeographical distribution patterns induced by temperature (Garcia-Pichel et
248 al., 2013; Couradeau et al., 2016). We found the thermotolerant cyanobacterial species *Microcoleus*
249 *steenstrupii* at our sampling sites, which may be related to the high mean annual temperature and
250 summer extreme temperatures (Garcia-Pichel et al., 2013). Continued expansion and intensification of
251 shrub encroachment across the Kalahari (e.g. Moleele et al., 2002; Tews et al., 2004; O'Connor et al.,
252 2014) will alter soil surface conditions, potentially favouring the species with lower temperature
253 thresholds. Given the increased relative abundance of *Microvirga* beneath shrubs (Fig. 5), our results
254 could suggest that shrub encroachment will lead to the potential replacement of carbon-fixing
255 cyanobacteria *Microcoleus* with nitrogen-fixing bacteria *Microvirga*, which lack the capacity for

256 photosynthesis.

257

258 ***4.2 Soil surface total carbon and total nitrogen***

259 Dryland soils are typically characterized by very low organic carbon and nitrogen contents, with
260 higher concentrations in the upper soil profile (Gao et al., 2010; Thomas et al., 2014). When biocrusts
261 form, they increase the amount of organic carbon and nitrogen in the uppermost millimetres of the soil
262 (Gao et al., 2010; Elbert et al., 2012). In our study, the total carbon and nitrogen content of the soil
263 surface samples varied with vegetation cover type, with higher concentrations found beneath shrubs
264 (Fig. 7). The carbon and nitrogen in the soil surface samples will likely have originated from various
265 sources, including cyanobacterial fixation, plant litter decomposition (Yan-Gui et al., 2013; Almagro et
266 al., 2015; Vikram et al., 2016), and inputs from wind-blown material and animal activities (Wezel et al.,
267 2000; Filazzola et al., 2017). In the biocrusts in grass areas, cyanobacteria accounted for 25-65% of the
268 bacterial communities (Fig. 3B) and are likely important participants in carbon fixation. In particular,
269 *Microcoleus steenstrupii*, as the most dominant cyanobacterial species, will play an important role in
270 the physical structure of the biocrust and associated soil nutrient cycle and storage. By contrast, the
271 lower relative abundances of *Microcoleus* and other photosynthetic cyanobacteria beneath shrubs
272 suggest that plant-driven inputs may be a greater source of soil carbon in these locations. Although we
273 have avoided using the term biocrust in relation to biologically crusted soil surfaces under shrubs
274 lacking large proportions of phototrophs, these soil surfaces are clearly part of a continuum and share
275 many properties in common with the phototrophic biocrusts found in grass areas. Current definitions of
276 biocrusts do not indicate where to draw a line between what is a biocrust and what is simply a soil

277 surface, and this is perhaps an issue for consideration in future research. As a contribution, our findings
278 suggest that shrub encroachment causes phototrophic biocrusts to alter their phylogenetic makeup, with
279 important functional implications. Although these communities may lose much of the capacity for
280 photosynthesis, we have shown that they retain or increase potential nitrogen fixation capacity, which
281 is a recognised biocrust function, and other biocrust properties like structural integrity are also retained.

282 In addition to the dominant species, some researchers suggest that non-dominant taxa may also play
283 potential ecosystem functions (e.g. Fuentes et al., 2016). For example, the genes of dominant
284 *Microvirga* related to nitrogen fixation have been reported as being obtained by horizontal gene transfer,
285 and thus some metabolic functions are required to uptake iron siderophores produced by other
286 neighbouring microbes (Bailey et al., 2014; Radl et al., 2014). Nevertheless, some species of chloroflexi
287 have been reported to photosynthetically grow by fixing CO_2 through a 3-hydroxypropionate pathway,
288 and some species of proteobacteria have an oxygen-producing photosynthetic pathway of photosystem
289 II (Lang and Oesterhelt, 1989; Boone and Castenholz, 2001; Bryant and Frigaard, 2006). Therefore,
290 both dominant and non-dominant bacterial compositions adjust biocrust carbon and nitrogen
291 metabolisms. Our results also demonstrate that there is a close relationship between the dominance of
292 soil surface bacterial OTUs and the overlying vegetation type (R^2>0.7). Bacterial species with a
293 specialized niche rather than a generalized lifestyle, are mainly restricted to soil surfaces beneath shrubs
294 (Fig. 4).

295 The abundance of cyanobacteria in soil surfaces samples is negatively related to total carbon and
296 total nitrogen contents (Figs. 8B, S2), which may be interpreted to infer that with the encroachment of
297 shrubs, more carbon and nitrogen would come from non-cyanobacterial fixation, such as litter
298 decomposition, other forms of microbial fixation, wind-blown sediments, and animal activities (Wezel

et al., 2000; Almagro et al., 2015; Filazzola et al., 2017). This is supported by our previous work in the Kalahari, which has shown that there is nutrient enrichment in wind-blown material and that there are significant differences in the carbon isotopic ratios of respired gases and litter from soils beneath shrubs and grasses (Thomas et al., 2018). Beneath shrubs, the increase and accumulation of carbon and nitrogen will form resource islands (Reynolds et al., 1999; Wang et al., 2009), which are not only beneficial to the metabolisms of heterotrophic microbial communities (Camargo-Ricalde and Dhillion, 2003), but also conducive to the growth and regeneration of shrubs (McAuliffe, 1988; Franco-Pizaña et al., 1995). Resource island formation provides a positive feedback mechanism to promote shrub establishment and growth at the expense of grasses. Nutrient cycling increasingly will be confined to litter accumulation zones beneath shrubs, leading to potentially undesirable hydrological and geomorphological changes (Parizek et al., 2002), including greater spatial heterogeneity of resources and more bare soil patches (Reynolds et al., 1999; D'Odorico et al., 2012), as well as loss of palatable herbaceous productivity (Ward, 2005). This feedback can be regarded as an internal, self-sustaining mechanism of shrub communities, and is difficult to reverse (D'Odorico et al., 2012), which helps to explain why shrub encroachment is commonly observed to be irreversible. Therefore, in those parts of the Kalahari and other drylands subject to shrub encroachment, the external factors driving and/or triggering such vegetation cover change should be identified (e.g. changing grazing, fire, erosion, or temperature regimes, or atmospheric CO_2 enrichment), and then possible management options to try and reverse or at least slow the shrub encroachment may be assessed. The interrelated and complex microbial mechanisms involved in sustaining shrub encroachment should be tested further with future studies looking at a wider range of vegetation, geographical areas and timespans.

5. Conclusion

Our study in the southwest Kalahari has revealed that vegetation cover type significantly affects the bacterial diversity and particularly the cyanobacterial abundance in the soil surface. The observed microbial community shifts infer that if the vegetation cover changes from grasses to shrubs, the abundance of cyanobacteria in the soil surface will decrease, reducing the photosynthetic capacity. The nitrogen fixation capacity, however, is likely to be retained or enhanced via other microbial groups. Our results show that soil surfaces beneath shrubs contain greater total carbon and total nitrogen contents than in grass areas, suggesting that non-cyanobacterial fixation, such as litter decomposition, other forms of microbial fixation, wind-blown sediments, and animal activities may be the main sources of carbon and nitrogen beneath shrubs. Hence, while shrub encroachment across the southwest Kalahari will promote carbon and nitrogen storage, it will likely inhibit cyanobacterial growth and biocrust development, and also lead to loss of palatable herbaceous productivity. Given the many positive ecological, hydrological and geomorphological functions of cyanobacterial biocrusts (Bowker, 2007; Zhao et al., 2014; Belnap et al., 2016), it would be beneficial to consider biocrust development, as well as grazing value, when implementing shrub encroachment control measures. As part of wider measures to support the social, economic and ecological significance of drylands and prevent or reverse dryland degradation (Millennium Ecosystem Assessment, 2005; Ezcurra, 2006), more consideration should be directed towards the development of biocrust conservation, management and rehabilitation schemes.

Acknowledgements

This study was kindly supported by the European Union's Horizon 2020 Research and Innovation

342 Programme under a Marie Skłodowska-Curie Grant (No. 663830), by the National Natural Science
343 Foundation of China (No. 31670456), and by the Youth Innovation Promotion Association of the
344 Chinese Academy of Sciences (No. 2017385). The paper was prepared while S. Lan was a Sêr Cymru
345 II Fellow at Aberystwyth University, and L. Wu was a Visiting Scholar at Aberystwyth University. We
346 thank the editor and three anonymous reviewers for the constructive comments that helped us to
347 improve the presentation and interpretation of our findings. The graphical abstract was created with
348 BioRender.com.

349

350 **Appendix A. Supplementary data**

351 Supplementary data for this article can be found online.

352

353 **References**

354 Adeel, Z., Safriel, U., Niemeijer, D., White, R., 2005. Ecosystems and human well-being: desertification
355 synthesis. World Resources Institute, Washington DC.
356 Almagro, M., Maestre, F.T., Martínez-López, J., Valencia, E., Reya, A., 2015. Climate change may
357 reduce litter decomposition while enhancing the contribution of photodegradation in dry perennial
358 Mediterranean grasslands. Soil Biology and Biochemistry 90, 214-223.
359 Bailey, A.C., Kellom, M., Poret-Peterson, A.T., Noonan, K., Hartnett, H.E., Raymond, J., 2014. Draft
360 genome sequence of *Microvirga* sp. strain BSC39, isolated from biological soil crust of Moab,
361 Utah. Genome Announc 2, e01197-14.
362 Belayneh, A., Tessema, Z.K., 2017. Mechanisms of bush encroachment and its inter-connection with

363 rangeland degradation in semi-arid African ecosystems: a review. Journal of Arid Land 9(2), 299-
364 312.
365 Belnap, J., Gillette, D.A., 1997. Disturbance of biological soil crusts: Impacts on potential wind
366 erodibility of sandy desert soils in southeastern Utah, Land Degradation and Development 8, 355-
367 362.
368 Belnap, J., Weber, B., Büdel, B., 2016. Biocrusts as an organizing principle in drylands. In: Weber, B.,
369 Büdel, B., Belnap, J. (eds.) Biological soil crusts: an organizing principle in drylands. Springer,
370 Berlin, pp 3-14.
371 Berdugo, M., Delgado-Baquerizo, M., Soliveres, S., Hernández-Clemente, R., Zhao, Y., Gaitán, J.J.,
372 Gross, N., Saiz, H., Maire, V., Lehmann, A., Rillig, M.C., Solé, R.V., Maestre, F.T., 2020. Global
373 ecosystem thresholds driven by aridity. Science, 14, 787-790
374 Boone, D.R., Castenholz, R.W. (eds), 2001. Bergey's Manual of Systematic Bacteriology (vol. 1),
375 Academic, New York.
376 Bowker, M.A., 2007. Biological soil crust rehabilitation in theory and practice: an underexploited
377 opportunity. Restoration Ecology 15, 13-23.
378 Bowker, M.A., Belnap, J., Büdel, B., Sannier, C., Pietrasiak, N., Eldridge, D.J., Rivera-Aguilar, V., 2016.
379 Controls on distribution patterns of biological soil crusts at micro- to global scale. In: Weber, B.,
380 Büdel, B., Belnap, J. (eds.), Biological soil crusts: an organizing principle in drylands. Springer,
381 Berlin, pp 173-198.
382 Briggs, A., Morgan, J.W., 2008. Morphological diversity and abundance of biological soil crusts differ
383 in relation to landscape setting and vegetation type. Australian Journal of Botany 56, 246-253.
384 Bryant, D.A., Frigaard, N.U., 2006. Prokaryotic photosynthesis and phototrophy illuminated. Trends in

385 Microbiology 14, 488-496.
386 Camargo-Ricalde, S.L., Dhillion, S.S., 2003. Endemic Mimosa species can serve as mycorrhizal
387 “resource islands” within semiarid communities of the Tehuacán-Cuicatlán Valley, Mexico.
388 Mycorrhiza 13, 129-136.
389 Couradeau, E., Karaoz, U., Chien Lim, H., Da Rocha, U.N., Northen, T., Brodie, E., García-Pichel, F.,
390 2016. Bacteria increase arid-land soil surface temperature through the production of sunscreens.
391 Nature Communication 7, 10373.
392 Deng, Y., Cui, X., Hernández, M., Dumont, M.G., 2014. Microbial diversity in hummock and hollow
393 soils of three wetlands on the Qinghai-Tibetan Plateau revealed by 16S rRNA pyrosequencing
394 PLoS One 9, e103115
395 D'Odorico, P., Okin, G.S., Bestelmeyer, B.T., 2012. A synthetic review of feedbacks and drivers of
396 shrub encroachment in arid grasslands. Ecohydrology 5, 520-530.
397 Dotaniya, M.L., Meena, V.D., 2015. Rhizosphere effect on nutrient availability in soil and its uptake by
398 plants: a review. Proceedings of the National Academy of Sciences, India Section B: Biological
399 Sciences 85, 1-12.
400 Edgar, R.C., 2013. UPARSE: highly accurate OTU sequences from microbial amplicon reads. Nature
401 Methods 10, 996-998.
402 Edgar, R.C., Haas, B.J., Clemente, J.C., Quince, C., Knight, R., 2011. UCHIME improves sensitivity
403 and speed of chimera detection. Bioinformatics 27, 2194-2200.
404 Elbert, W., Weber, B., Burrows, S., Steinkamp, J., Büdel, B., Andreae, M., Pöschl, U., 2012.
405 Contribution of cryptogamic covers to the global cycles of carbon and nitrogen. Nature Geoscience
406 5(7), 459-462.

Eldridge, D.J., Bowker, M.A., Maestre, F.T., Roger, E., Reynolds, J.F., Whitford, W.G., 2011. Impacts of shrub encroachment on ecosystem structure and functioning: towards a global synthesis. Ecology Letters 14, 709-722.

Eldridge, D.J., Maestre, F.T., Maltez-Mouro, S., Bowker, M.A., 2012. A global database of shrub encroachment effects on ecosystem structure and functioning. Ecology 93, 2499.

Elliott, D.R., Thomas, A.D., Hoon, S.R., Sen, R., 2014. Niche partitioning of bacterial communities in biological crusts and soils under grasses, shrubs and trees in the Kalahari. Biodiversity and Conservation 23, 1709-1733.

Elliott, D.R., Thomas, A.D., Strong, C.L., Bullard, J., 2019. Surface stability in drylands is influenced by dispersal strategy of soil bacteria. Journal of Geophysical Research: Biogeosciences, 124(11), 3403-3418.

Ezcurra, E., (ed.) 2006. Global Deserts Outlook. United Nations Environment Programme, Nairobi, Kenya.

Filazzola, A., Westphal, M., Powers, M., Liczner, A.R., Woollett, D.A.S., Johnson, B., Lortie, C.J., 2017. Non-trophic interactions in deserts: facilitation, interference, and an endangered lizard species. Basic and Applied Ecology 20, 51-61.

Food and Agriculture Organisation (FAO), 2015. World reference base for soil. Resources 2014. International soil classification system for naming soils and creating legends for soil maps. World Soil Resources Reports No. 106, Rome, FAO.

Franco-Pizaña, J., Fulbright, T.E., Gardiner, D.T., 1995. Spatial relations between shrubs and Prosopis glandulosa canopies. Journal of Vegetation Science 6, 73-78.

Fuentes, S., Barra, B., Caporaso, J.G., Seeger, M., 2016. From rare to dominant: A fine-tuned soil

bacterial bloom during petroleum hydrocarbon bioremediation. Applied Environmenal Microbiology 82, 888-896.

Gao, S., Ye, X., Chu, Y., Dong, M., 2010. Effects of biological soil crusts on profile distribution of soil water, organic carbon and total nitrogen in Mu Us Sandland, China. Journal of Plant Ecology 3(4), 279-284.

Garcia-Pichel, F., Pringault, O., 2001. Cyanobacteria track water in desert soils. Nature 413, 380-381.

Garcia-Pichel, F., Loza, V., Marusenko, Y., Mateo, P., Potrafka, R.M., 2013. Temperature drives the continental-scale distribution of key microbes in topsoil communities. Science 340, 1574-1577.

Giraldo-Silva, A., Fernandes, V.M.C., Bethany, J., Garcia-Pichel, F., 2020. Niche Partitioning with Temperature among Heterocystous Cyanobacteria (Scytonema spp., Nostoc spp., and Tolypothrix spp.) from Biological Soil Crusts. Microorganisms 8(3), 396

Howe, E.A., Sinha, R., Schlauch, D., Quackenbush, J., 2011. RNA-Seq analysis in MeV. Bioinformatics 27(22), 3209-3210.

Hu, C., Liu, Y., 2003. Primary succession of algal community structure in desert soil. Acta Botanica Sinica 45, 917-924.

Hu, C., Gao, K., Whitton, B.A., 2012. Semi-arid Regions and Deserts. In Whitton B.A. (ed.) Ecology of Cyanobacteria II: Their Diversity in Space and Time. Springer Science + Business Media, Dordrecht, pp: 345-369.

Huang, J., Yu, H., Guan, X., Wang, G., Guo, R., 2016. Accelerated dryland expansion under climate change. Nature Climate Change 6, 166-171.

Komárek, J., Kaštovský, J., Mareš, J., Johansen, J.R., 2014. Taxonomic classification of cyanoprokaryotes (cyanobacterial genera) 2014, using a polyphasic approach. Preslia 86, 295-335.

451 Lan, S., Wu, L., Zhang, D., Hu, C., 2012. Successional stages of biological soil crusts and their
452 microstructure variability in Shapotou region (China). Environmental Earth Sciences 65(1), 77-88.
453 Lan, S., Zhang, Q., Wu, L., Liu, Y., Zhang, D., Hu, C., 2014a. Artificially accelerating the reversal of
454 desertification: cyanobacterial inoculation facilitates the succession of vegetation communities.
455 Environmental Science and Technology 48, 307-315.
456 Lan, S., Wu, L., Zhang, D., Hu, C., 2014b. Desiccation provides photosynthetic protection for crust
457 cyanobacteria *Microcoleus vaginatus* from high temperature. Physiologia Plantarum 152, 35-354.
458 Lan, S., Wu, L., Zhang, D., Hu, C., 2015. Effects of light and temperature on open cultivation of desert
459 cyanobacterium *Microcoleus vaginatus*. Bioresource Technology 182, 144-150.
460 Lang, F., Oesterhelt, D., 1989. Microaerophilic growth and induction of the photosynthetic reaction
461 center in *Rhodopseudomonas viridis*. Journal of Bacteriology 171, 2827-2834.
462 Leakey, A.D.B., Ainsworth, E.A., Bernacchi, C.J., Rogers, A., Long, S.P., Ort, D.R., 2009. Elevated
463 CO_2 effects on plant carbon, nitrogen, and water relations: Six important lessons from FACE.
464 Journal of Experimental Botany 60(10), 2859-2876.
465 Li, X., He, M., Zerbe, S., Li, X., Liu, L., 2010. Micro-geomorphology determines community structure
466 of biological soil crusts at small scales. Earth Surface Processes and Landforms 35, 932-940.
467 Li, X., Jia, R., Chen, Y., Huang, L., Zhang, P., 2011. Association of ant nests with successional stages
468 of biological soil crusts in the Tengger Desert, Northern China. Applied Soil Ecology 47, 59-66.
469 Luo, J., Liang, H., Yan, L., Ma, J., Yang, Y., Li, G., 2013. Microbial community structures in a closed
470 raw water distribution system biofilm as revealed by 454-pyrosequencing analysis and the effect
471 of microbial biofilm communities on raw water quality. Bioresource Technology 148, 189-195.
472 Machado-de-Lima, N.M., Fernandes, V.M.C., Roush, D., Velasco Ayuso, S., Rigonato, J., Garcia-Pichel,

F., Branco, L.H.Z., 2019. The compositionally distinct cyanobacterial biocrusts from Brazilian savanna and their environmental drivers of community diversity. Frontiers in Microbiology 10, 2798.

Maestre, F.T., Bowker, M.A., Puche, M.D., Hinojosa, M.B., Martínez, I., García-Palacios, P., Castillo, A.P., Soliveres, S., Luzuriaga, A.L., Sánchez, A.M., Carreira, J.A., Gallardo, A., Escudero, A., 2009. Shrub encroachment can reverse desertification in Mediterranean semiarid grasslands. Ecology Letters 12, 930-941.

Maestre, F.T., Eldridge, D.J., Soliveres, S., Kéfi, S., Delgado-Baquerizo, M., Bowker, M.A., García-Palacios, P., Gaitán, J., Gallardo, A., Lázaro, R., Berdugo, M., 2016. Structure and functioning of dryland ecosystems in a changing world. Annual Review of Ecology, Evolution, and Systematics, 47(1), 215-237.

Mager, D.M., Thomas, A.D., 2011. Extracellular polysaccharides from cyanobacterial soil crusts: a review of their role in dryland soil processes. Journal of Arid Environments 75(2), 91-97.

Maier, S., Tamm, A., Wu, D., Caesar, J., Grube, M., Weber, B., 2018. Photoautotrophic organisms control microbial abundance, diversity, and physiology in different types of biological soil crusts. ISME Journal 12, 1032-1046.

Martínez, I., Ecudero, A., Maestre, F.T., de la Cruz, A., Guerrero, C., Rubio, A., 2006. Small-scale patterns of abundance of mosses and lichens forming biological soil crusts in two semi-arid gypsum environments. Australian Journal of Botany 54, 339-348.

McAuliffe, J.R., 1988. Markovian dynamics of simple and complex desert plant communities. American Naturalist 131, 459-490.

Millennium Ecosystem Assessment, 2005. Millennium Ecosystem Assessment Synthesis Report. Island

Press, Washington, D.C. http://www.millenniumassessment.org/en/Synthesis.aspx.

Moleele, N.M., Ringrose, S., Matheson, W., Vanderpost, C., 2002. More woody plants? the status of bush encroachment in Botswana's grazing areas. Journal of Environmental Management, 64(1), 3-11.

Muñoz-Martín, M.Á., Becerra-Absalón, I., Perona, E., Fernández-Valbuena, L., Garcia-Pichel, F., Mateo, P., 2019. Cyanobacterial biocrust diversity in Mediterranean ecosystems along a latitudinal and climatic gradient. New Phytologist 221, 123-141.

O'Connor, T.G., Puttick, J.R., Hoffman, M.T., 2014. Bush encroachment in southern Africa: changes and causes. African Journal of Range and Forage Science 31, 67-88.

Parizek, B., Rostagno, C.M., Sottini. R., 2002. Soil erosion as affected by shrub encroachment in northeastern Patagonia. Journal of Range Management 55, 43-48.

Radl, V., Simões-Araújo, J.L., Leite, J., Passos, S.R., Martins, L.M.V., Xavier, G.R., Rumjanek, N.G., Baldani, J.I., Zilli, J.E., 2014. *Microvirga vignae* sp. nov., a root nodule symbiotic bacterium isolated from cowpea grown in the semi-arid of Brazil. International Journal of Systematic and Evolutionary Microbiology 64, 725-730.

Reynolds, J.F., Smith, D.M.S., Lambin, E.F., Turner II, B.L., Mortimore, M., Batterbury, S.P.J., Downing, T.E., Dowlatabadi, H., Fernández, R.J., Herrick, J.E., Huber-Sannwald, E., Jiang, H., Leemans, R., Lynam, T., Maestre, F.T., Ayarza, M., Walker, B., 2007. Global desertification: Building a science for dryland development. Science 316, 847-851.

Reynolds, J.F., Virginia, R.A., Kemp, P.R., de Soyza, A.G., Tremmel, D.C., 1999. Impact of drought on desert shrubs: effects of seasonality and degree of resource island development. Ecological Monographs 69, 69-106.

517 Rossi-Tamisier, M., Benamar, S., Raoult, D., Fournier, P.E., 2015. Cautionary tale of using 16S rRNA
518 gene sequence similarity values in identification of human-associated bacterial species.
519 International Journal of Systematic and Evolutionary Microbiology 65, 1929-1934.
520 Sankaran, M., Hanan, N.P., Scholes, R.J., et al., 2005. Determinants of woody cover in African savannas.
521 Nature 438(7069), 846-849.
522 Stevens, N., Lehmann, C.E., Murphy, B.P., Durigan, G., 2017. Savanna woody encroachment is
523 widespread across three continents. Global Change Biology 23, 235-244.
524 Swenson, T.L., Karaoz, U., Swenson, J.M., Bowen, B.P., Northen, T.R., 2018. Linking soil biology and
525 chemistry in biological soil crust using isolate exometabolomics. Nature Communication 9, 19
526 Tamura, K., Stecher, G., Peterson, D., Filipski, A., Kumar, S., 2013. MEGA 6: molecular evolutionary
527 genetics analysis version 6.0. Molecular Biology and Evolution 30, 2725-2729.
528 Tews, J. Schurr, F., Jeltsch F., 2004. Seed dispersal by cattle may cause shrub encroachment of *Grewia*
529 *flava* on southern Kalahari rangelands. Applied Vegetation Science 7, 89-102.
530 Thiet, R.K., Doshas, A., Smith, S.M., 2014. Effects of biocrusts and lichen-moss mats on plant
531 productivity in a US sand dune ecosystem. Plant and Soil 377, 235-244.
532 Thomas, A.D., 2012. Impact of grazing intensity on seasonal variations of soil organic carbon and soil
533 CO_2 efflux in two semi-arid grasslands in southern Botswana. Philosophical Transactions of the
534 Royal Society B, 367, 3076-3086.
535 Thomas, A.D., Dougill, A.J., 2007. Spatial and temporal distribution of cyanobacterial soil crusts in the
536 Kalahari: implications for soil surface properties. Geomorphology, 85, 17-29
537 Thomas, A.D., Dougill, A.J., Elliott D.R., Mairs H., 2014. Seasonal differences in soil CO_2 efflux and
538 carbon storage in Ntwetwe Pan, Makgadikgadi Basin, Botswana. Geoderma 219-220, 72-81.

539 Thomas, A.D., Elliott, D.R., Dougill, A.J., Stringer, L.C., Hoon, S.R., Sen, R., 2018. The influence of
540 trees, shrubs, and grasses on microclimate, soil carbon, nitrogen, and CO_2 efflux: Potential
541 implications of shrub encroachment for Kalahari rangelands. Land Degradation and Development
542 29, 1306-1316.
543 UNESCO, 2016. Stampriet Transboundary Aquifer System Assessment: governance of Groundwater
544 resources in Transboundary Aquifers (GRETA), phase 1: technical report.
545 Urbanová, M., Šnajdr, J., Baldrian, P., 2015. Composition of fungal and bacterial communities in forest
546 litter and soil is largely determined by dominant trees. Soil Biology and Biochemistry 84, 53-64.
547 Van Auken, O.W., 2009. Causes and consequences of woody plant encroachment into western North
548 American grasslands. Journal of Environmental Management 90(10), 2931-2942.
549 Vikram, S., Guerrero, L.D., Makhalanyane, T.P., Le, P.T., Seely, M., Cowan, D.A., 2016. Metagenomic
550 analysis provides insights into functional capacity in a hyperarid desert soil niche community.
551 Environmental Microbiology 18, 1875-1888.
552 Wang, Q., Garrity, G.M., Tiedje, J.M., Cole, J.R., 2007. Naive Bayesian classifier for rapid assignment
553 of rRNA sequences into the new bacterial taxonomy. Applied and Environmental Microbiology
554 73, 5261-5267.
555 Wang, L., D'Odorico, P., Manzoni, S., Porporato, A., Macko, S., 2009. Soil carbon and nitrogen
556 dynamics in southern African savannas: The effect of vegetation-induced patch-scale
557 heterogeneities and large scale rainfall gradients. Climate Change 94, 63-76.
558 Ward, D., 2005. Do we understand the causes of bush encroachment in African savannas? African
559 Journal of Range and Forage Science 22, 101-105.
560 Weon, H.Y., Kwon, S.W., Son, J.A., Jo, E.H., Kim, S.J., Kim, Y.S., Kim, B.Y., Ka, J.O., 2010.

561 Description of *Microvirga aerophila* sp. nov. and *Microvirga aerilata* sp. nov., isolated from air,
562 reclassification of *Balneimonas flocculans takeda*, et al. 2004 as *Microvirga flocculans comb* nov.
563 and emended description of the genus *Microvirga*. International Journal of Systematic and
564 Evolutionary Microbiology 60(11), 2596-2600.
565 Wezel, A., Rajot, J.L., Herbrig, C., 2000. Influence of shrubs on soil characteristics and their function
566 in Sahelian agro-ecosystems in semi-arid Niger. Journal of Arid Environments 44, 383-398.
567 Yan-Gui, S., Xin-Rong, L., Ying-Wu, C., Zhi-Shan, Z., Yan, L., 2013. Carbon fixation of
568 cyanobacterial-algal crusts after desert fixation and its implication to soil organic matter
569 accumulation in desert. Land Degradation and Development 24, 342-349.
570 Zhang, Y., Wang, H., Wang, X., Yang, W., Zhang, D., 2006. The microstructure of microbiotic crust and
571 its influence on wind erosion for a sandy soil surface in the Gurbantunggut Desert of Northwestern
572 China. Geoderma 132, 441-449.
573 Zhang, Z., Li X., Nowak, R.S., Wu, P., Gao, Y., Zhao, Y., Huang, L., Hu, Y., Jia, R., 2013. Effect of
574 sand–stabilizing shrubs on soil respiration in a temperate desert. Plant and Soil 367, 449-463.
575 Zhao, Y., Qin, N., Weber, B., Xu, M., 2014. Response of biological soil crusts to raindrop erosivity and
576 underlying influences in the hilly Loess Plateau region, China. Biodiversity and Conservation 23,
577 1669-1686.

Table 1. Soil surface sampling habitats and the basic properties, as derived by gene sequencing

Sample*	Sampling season	Vegetation cover type	Dominant species	OTU number	Good's Coverage (%)
ELM	March	Perennial grass	*Eragrostis lehmanniana*	104-182	95.3 ± 1.4
ELN	November	Perennial grass	*Eragrostis lehmanniana*	121-158	98.1 ± 1.9
SKM	March	Annual grass	*Schmidtia kalahariensis*	160-226	98.7 ± 0.8
SKN	November	Annual grass	*Schmidtia kalahariensis*	166-220	98.0 ± 0.5
GFM	March	Shrub	*Grewia flava*	173-219	96.0 ± 1.4
GFN	November	Shrub	*Grewia flava*	153-251	95.8 ± 2.6

* in the sample codes, the first two letters (EL, SK, GF) represent samples from areas of *Eragrostis lehmanniana*, *Schmidtia kalahariensis* and *Grewia flava*, respectively, and the last letter (M, N) represents samples from March and November, respectively. For each vegetation cover type, and in each sampling season, soil surface samples were collected from three independent sites.

Figure captions:

Fig. 1 A) The study location in the southwest Kalahari showing the extent of Kalahari Sands and isohyets of mean annual precipitation. B) The upper profile of Kalahari Sand with a well-developed biocrust. C) Annual grass *Schmidtia kalahariensis*. D) Perennial grass *Eragrostis lehmanniana*. E) Shrub *Grewia flava* (modified after Elliott et al., 2014 and Thomas et al., 2018).

Fig. 2 Comparison of photosynthetically active radiation (PAR; A and B) and soil surface temperature (C and D) associated with grass and shrub covers. (A) and (C): November 2011; (B) and (D): March 2012. The box and solid line present the 25th, 50th and 75th percentiles with mean values marked as dotted lines, while error bars present the 5th and 95th percentiles. For each variable, the different letters indicate that the difference is significant at 0.05 level (P <0.05).

Fig. 3 Bacterial community compositions, diversity and cyanobacterial abundance in soil surface samples from the different vegetation cover types and different sampling seasons: A) bacterial community structure (mean relative abundance) showing the similarity of bacterial compositions at phylum level; B) cyanobacterial abundances (mean ± SD); and C) the rarefaction curves of Shannon index (mean). ELM: *E. lehmanniana* (March); ELN: *E. lehmanniana* (November); SKM: *S. kalahariensis* (March); SKN: *S. kalahariensis* (November); GFM: *G. flava* (March); GFN: *G. flava* (November).

Fig. 4 A) Venn diagram showing the distribution of OTUs in soil surface samples associated with the different vegetation cover types; B) the relationships between mean OTU relative abundance and frequency of occurrence. Each dot represents an OTU, but a few OTUs with higher relative abundance are not displayed in order to show the majority of OTUs in a clear pattern. The red symbols indicate cyanobacterial OTUs, while the black symbols indicate the other bacterial OTUs.

Fig. 5 Dominant bacterial phylogenetic identification and relationship with soil surface samples: A) maximum-likelihood tree of the dominant bacterial OTUs based on 16S rRNA gene sequences. OTU-x indicates the dominant bacterial OTUs in our study, and the text in brackets shows the Genbank accession numbers of the sequences from other studies; B) circos plot showing the mean relative

abundance (%) of dominant species associated with the different vegetation covers. ELM: *E. lehmanniana* (March); ELN: *E. lehmanniana* (November); SKM: *S. kalahariensis* (March); SKN: *S. kalahariensis* (November); GFM: *G. flava* (March); GFN: *G. flava* (November).

Fig. 6 Maximum-likelihood tree of the cyanobacterial OTUs based on 16S rRNA gene sequences. Bootstrap values >40% are shown beside the branches. OTU-x indicates the cyanobacterial OTUs in our study, and the text in brackets shows the Genbank accession numbers of the different cyanobacterial species.

Fig. 7 Total carbon (A) and total nitrogen contents (B) in the different soil surface samples (mean ± SD). For each variable, the values with different letters indicate that the difference is significant between the different vegetation cover types (P <0.05): a: *E. lehmanniana* (EL); b: *S. kalahariensis* (SK); c: *G. flava* (GF). ELM: *E. lehmanniana* (March); ELN: *E. lehmanniana* (November); SKM: *S. kalahariensis* (March); SKN: *S. kalahariensis* (November); GFM: *G. flava* (March); GFN: *G. flava* (November).

Fig. 8 Relationships between total carbon content, total nitrogen content and cyanobacterial abundance in the soil surface samples associated with the three vegetation cover types: A) scatter plot showing that the ratio of total carbon to total nitrogen is similar across all three vegetation covers; B) scatter plot showing that cyanobacterial abundance decreases with increasing total carbon content.

Fig. 1.

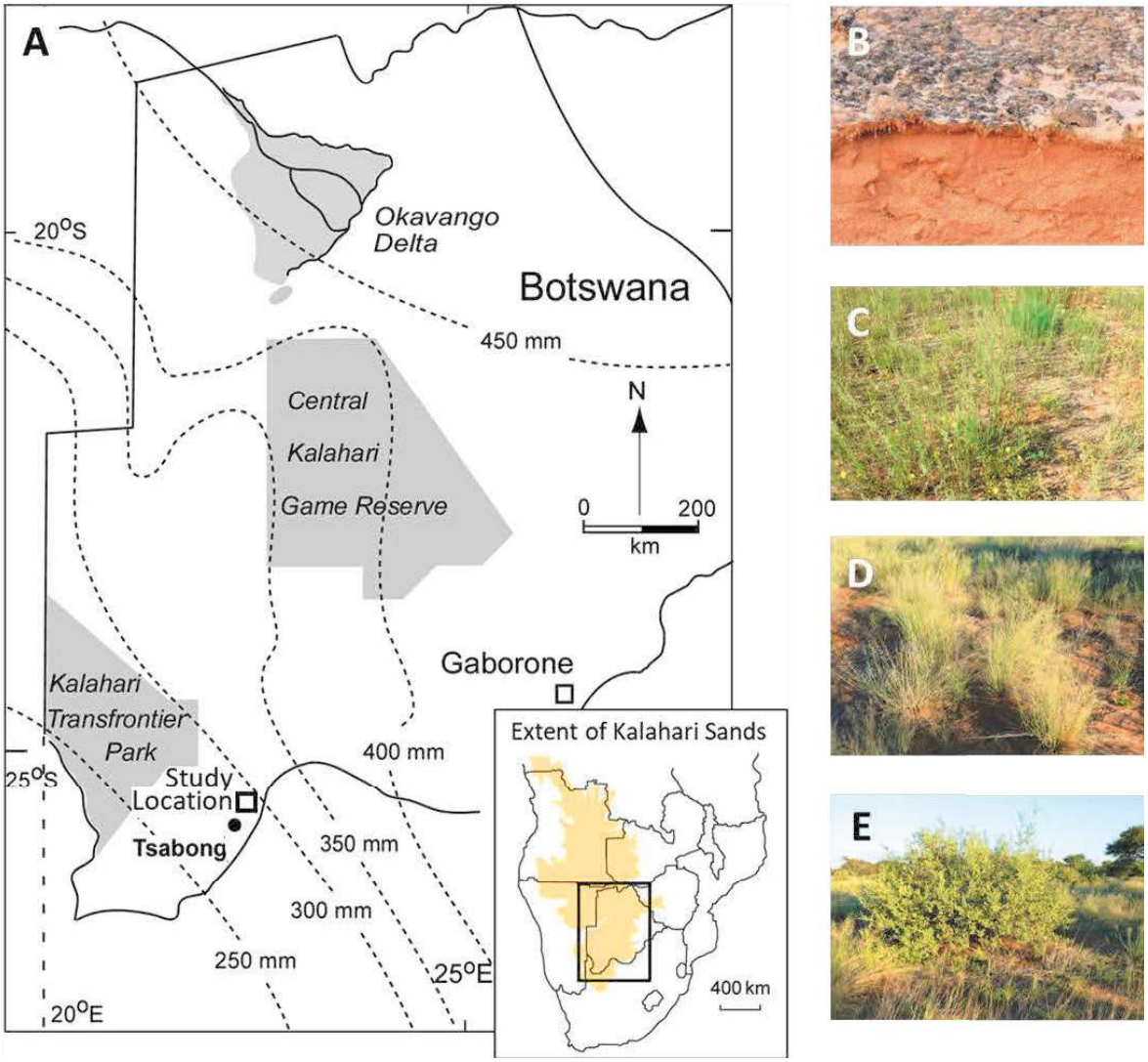
A
20°S
Okavango
Delta
Botswana
450 mm
Central
Kalahari
Game Reserve
N
0
200
km
Gaborone
Kalahari
Transfrontier
Park
400 mm
25°S
Study
Location
Tsabong
350 mm
300 mm
250 mm
25°E
20°E
Extent of Kalahari Sands
400 km
B
C
D
E

Fig. 2.

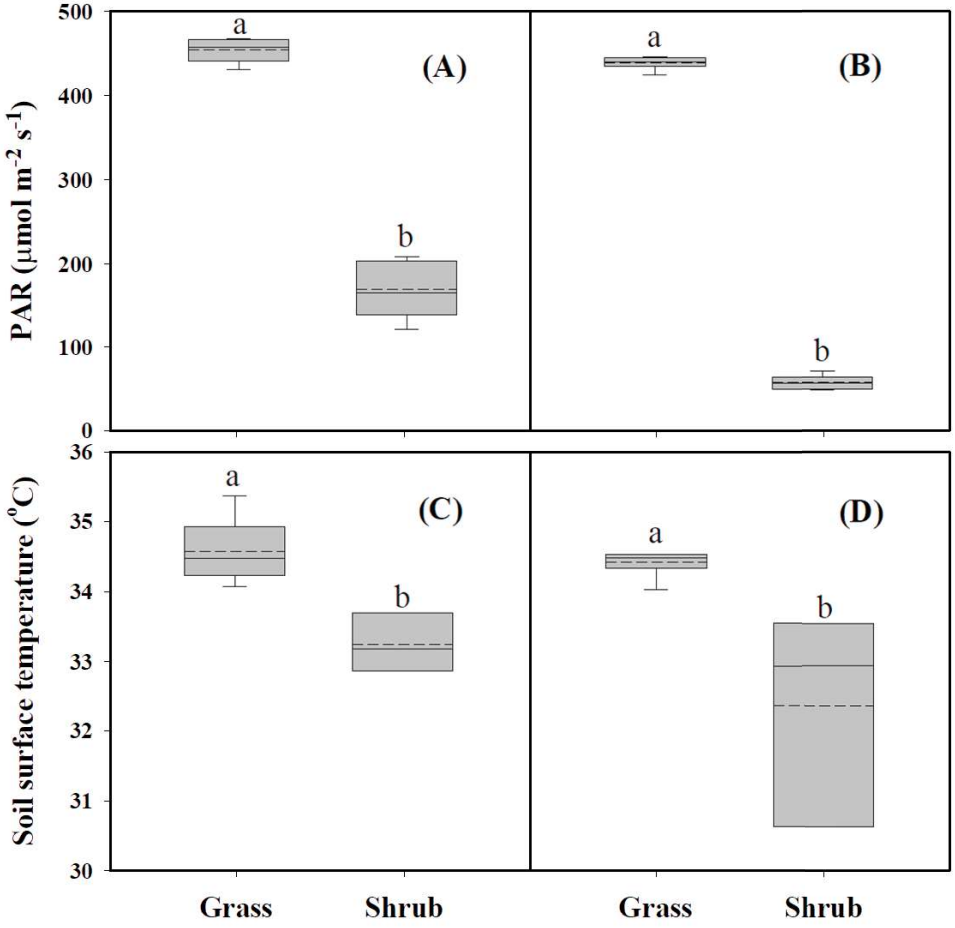
PAR (µmol m-2 s-1)
Soil surface temperature (°C)
(A)
(B)
(C)
(D)
a
b
Grass
Shrub

Fig. 3

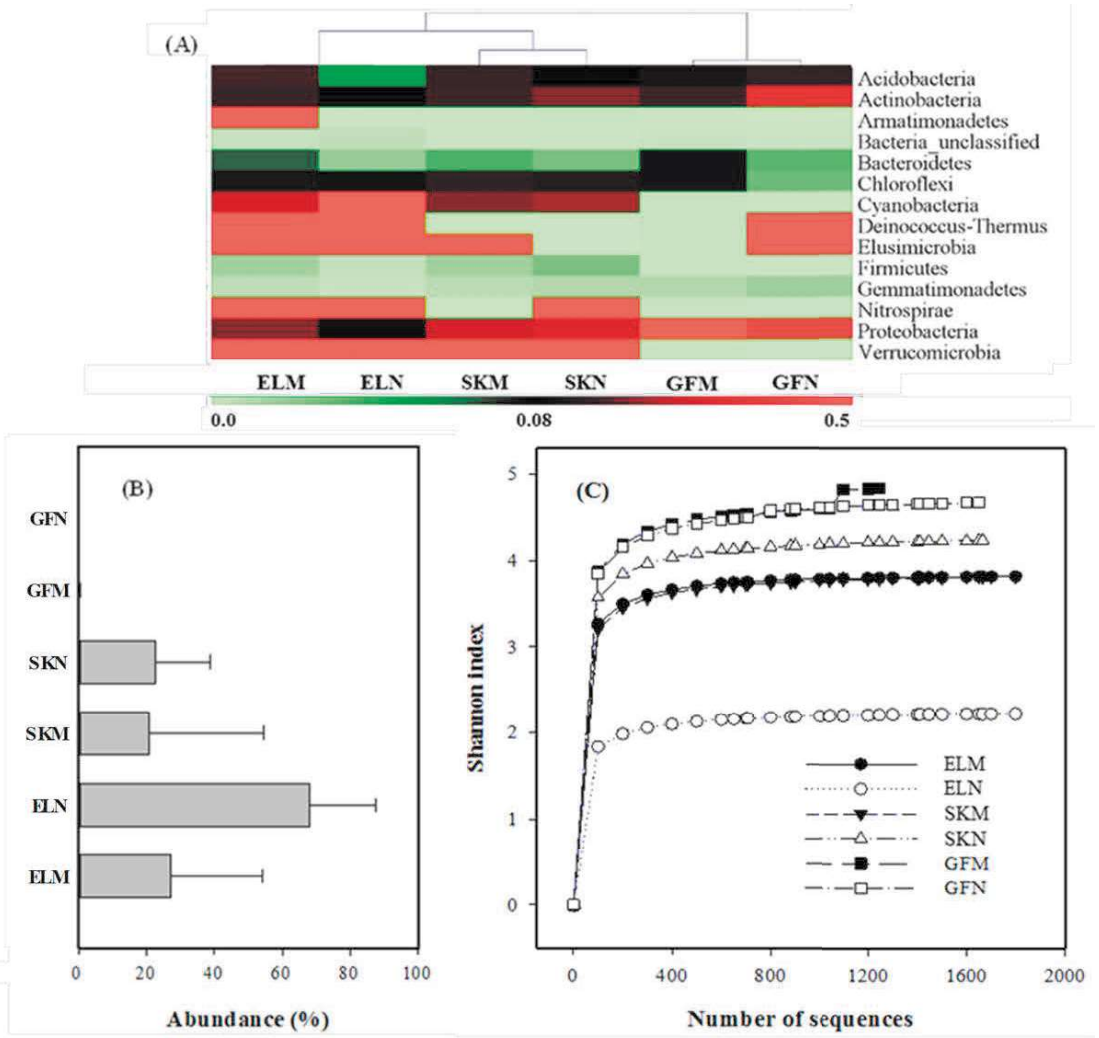
(A)
Acidobacteria
Actinobacteria
Armatimonadetes
Bacteria_unclassified
Bacteroidetes
Chloroflexi
Cyanobacteria
Deinococcus-Thermus
Elusimicrobia
Firmicutes
Gemmatimonadetes
Nitrospirae
Proteobacteria
Verrucomicrobia
ELM ELN SKM SKN GFM GFN
0.0
0.08
0.5
(B)
GFN
GFM
SKN
SKM
ELN
ELM
0 20 40 60 80 100
Abundance (%)
(C)
Shannon index
0 1 2 3 4 5
0 400 800 1200 1600 2000
Number of sequences
ELM
ELN
SKM
SKN
GFM
GFN

Fig. 4

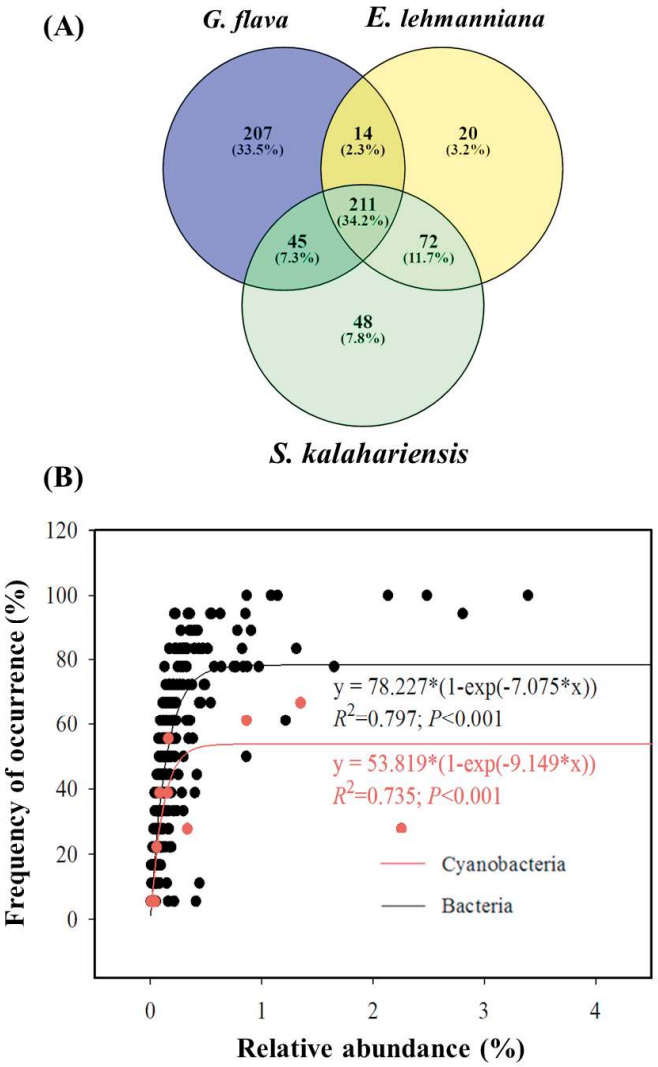
(A)
G. flava
E. lehmanniana
207
(33.5%)
14
(2.3%)
20
(3.2%)
211
(34.2%)
45
(7.3%)
72
(11.7%)
48
(7.8%)
S. kalahariensis
(B)
Frequency of occurrence (%)
Relative abundance (%)
y = 78.227*(1-exp(-7.075*x))
R2=0.797; P<0.001
y = 53.819*(1-exp(-9.149*x))
R2=0.735; P<0.001
Cyanobacteria
Bacteria

Fig. 5

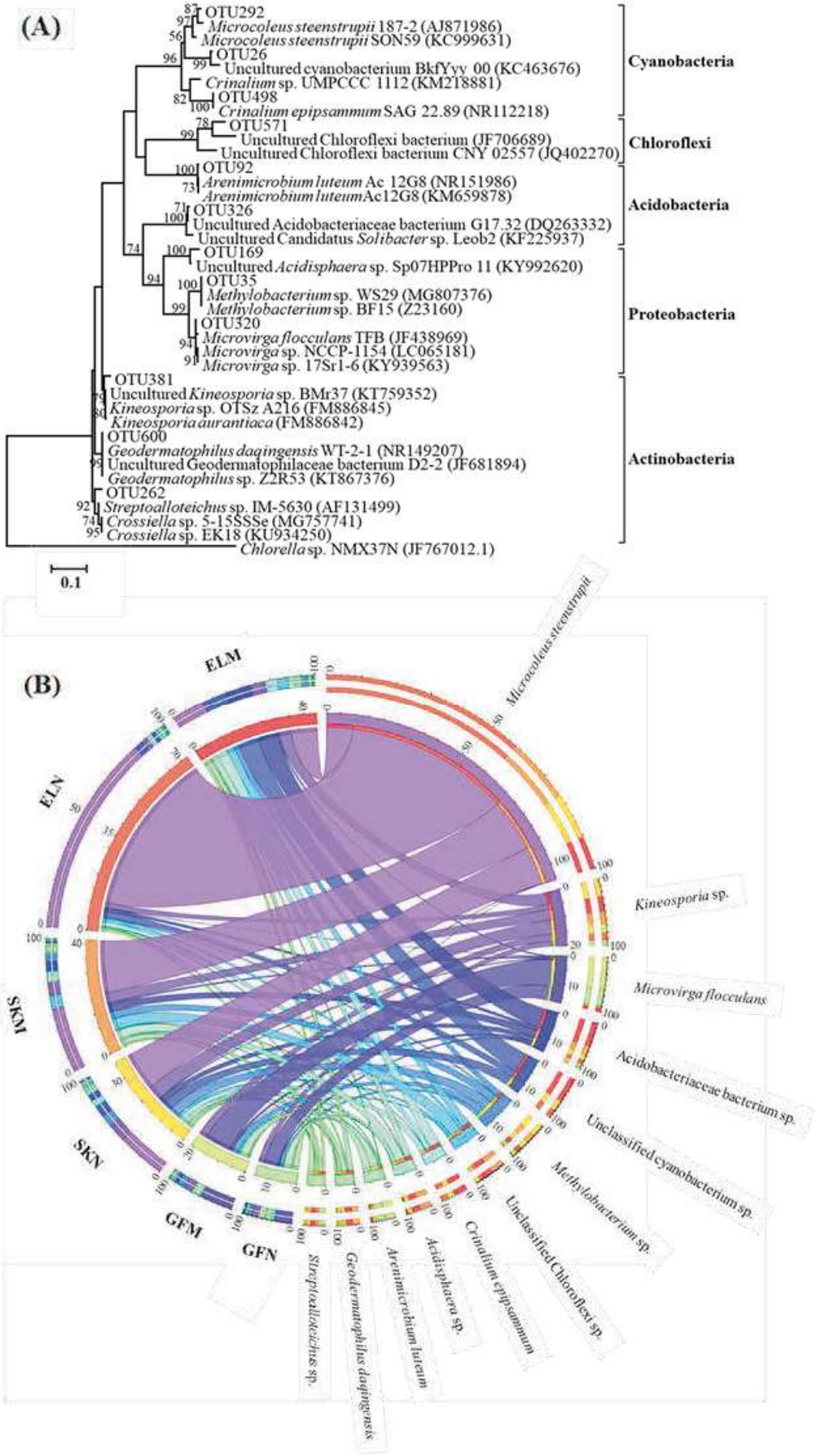
(A)
OTU292
Microcoleus steenstrupii 187-2 (AJ871986)
Microcoleus steenstrupii SON59 (KC999631)
OTU26
Uncultured cyanobacterium BkfYyy 00 (KC463676)
Crinalium sp. UMPCCC 1112 (KM218881)
OTU498
Crinalium epipsammum SAG 22.89 (NR112218)
OTU571
Uncultured Chloroflexi bacterium (JF706689)
Uncultured Chloroflexi bacterium CNY 02557 (JQ402270)
OTU92
Arenimicrobium luteum Ac 12G8 (NR151986)
Arenimicrobium luteum Ac12G8 (KM659878)
OTU326
Uncultured Acidobacteriaceae bacterium G17.32 (DQ263332)
Uncultured Candidatus Solibacter sp. Leob2 (KF225937)
OTU169
Uncultured Acidisphaera sp. Sp07HPPro 11 (KY992620)
OTU35
Methylobacterium sp. WS29 (MG807376)
Methylobacterium sp. BF15 (Z23160)
OTU320
Microvirga flocculans TFB (JF438969)
Microvirga sp. NCCP-1154 (LC065181)
Microvirga sp. 17Sr1-6 (KY939563)
OTU381
Uncultured Kineosporia sp. BMr37 (KT759352)
Kineosporia sp. OTSz A216 (FM886845)
Kineosporia aurantiaca (FM886842)
OTU600
Geodermatophilus daqingensis WT-2-1 (NR149207)
Uncultured Geodermatophilaceae bacterium D2-2 (JF681894)
Geodermatophilus sp. Z2R53 (KT867376)
OTU262
Streptoalloteichus sp. IM-5630 (AF131499)
Crossiella sp. 5-15SSSe (MG757741)
Crossiella sp. EK18 (KU934250)
Chlorella sp. NMX37N (JF767012.1)
0.1
Cyanobacteria
Chloroflexi
Acidobacteria
Proteobacteria
Actinobacteria
(B)
ELM
ELN
SKM
SKN
GFM
GFN
Microcoleus steenstrupii
Kineosporia sp.
Microvirga flocculans
Acidobacteriaceae bacterium sp.
Unclassified cyanobacterium sp.
Methylobacterium sp.
Unclassified Chloroflexi sp.
Crinalium epipsammum
Acidisphaera sp.
Arenimicrobium luteum
Geodermatophilus daqingensis
Streptoalloteichus sp.

Fig. 6

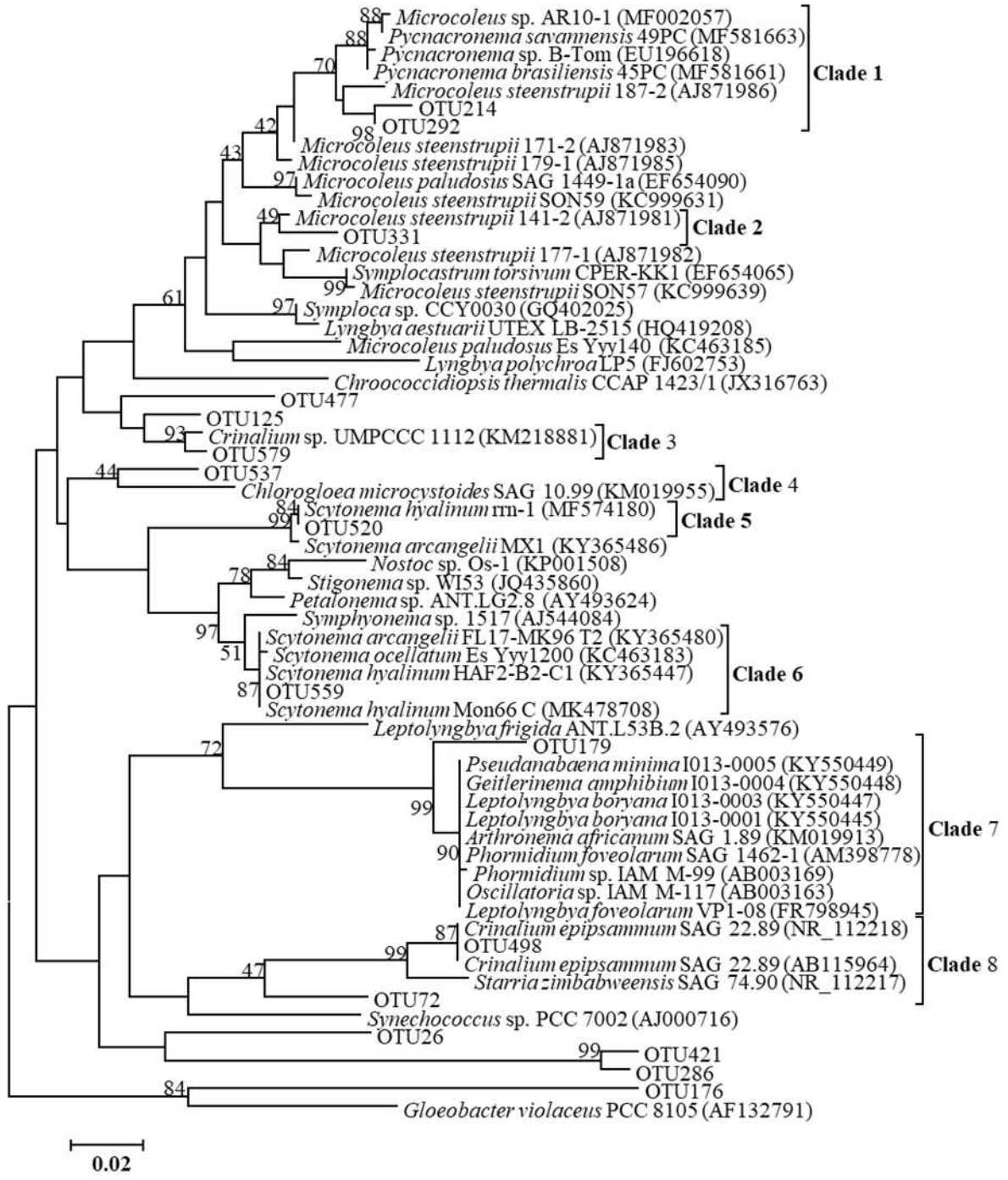
Microcoleus sp. AR10-1 (MF002057)
Pycnacronema savannensis 49PC (MF581663)
Pycnacronema sp. B-Tom (EU196618)
Pycnacronema brasiliensis 45PC (MF581661)
Microcoleus steenstrupii 187-2 (AJ871986)
OTU214
OTU292
Clade 1
Microcoleus steenstrupii 171-2 (AJ871983)
Microcoleus steenstrupii 179-1 (AJ871985)
Microcoleus paludosus SAG 1449-1a (EF654090)
Microcoleus steenstrupii SON59 (KC999631)
Microcoleus steenstrupii 141-2 (AJ871981)
OTU331
Clade 2
Microcoleus steenstrupii 177-1 (AJ871982)
Symplocastrum torsivum CPER-KK1 (EF654065)
Microcoleus steenstrupii SON57 (KC999639)
Symploca sp. CCY0030 (GQ402025)
Lyngbya aestuarii UTEX LB-2515 (HQ419208)
Microcoleus paludosus Es Yyy140 (KC463185)
Lyngbya polychroa LP5 (FJ602753)
Chroococcidiopsis thermalis CCAP 1423/1 (JX316763)
OTU477
OTU125
Crinalium sp. UMPCCC 1112 (KM218881)
OTU579
Clade 3
OTU537
Chlorogloea microcystoides SAG 10.99 (KM019955)
Clade 4
Scytonema hyalinum rrn-1 (MF574180)
OTU520
Scytonema arcangelii MX1 (KY365486)
Clade 5
Nostoc sp. Os-1 (KP001508)
Stigonema sp. WI53 (JQ435860)
Petalonema sp. ANT.LG2.8 (AY493624)
Symphyonema sp. 1517 (AJ544084)
Scytonema arcangelii FL17-MK96 T2 (KY365480)
Scytonema ocellatum Es Yyy1200 (KC463183)
Scytonema hyalinum HAF2-B2-C1 (KY365447)
OTU559
Scytonema hyalinum Mon66 C (MK478708)
Clade 6
Leptolyngbya frigida ANT.L53B.2 (AY493576)
OTU179
Pseudanabaena minima I013-0005 (KY550449)
Geitlerinema amphibium I013-0004 (KY550448)
Leptolyngbya boryana I013-0003 (KY550447)
Leptolyngbya boryana I013-0001 (KY550445)
Arthronema africanum SAG 1.89 (KM019913)
Phormidium foveolarum SAG 1462-1 (AM398778)
Phormidium sp. IAM M-99 (AB003169)
Oscillatoria sp. IAM M-117 (AB003163)
Leptolyngbya foveolarum VP1-08 (FR798945)
Clade 7
Crinalium epipsammum SAG 22.89 (NR_112218)
OTU498
Crinalium epipsammum SAG 22.89 (AB115964)
Starria zimbabweensis SAG 74.90 (NR_112217)
Clade 8
OTU72
Synechococcus sp. PCC 7002 (AJ000716)
OTU26
OTU421
OTU286
OTU176
Gloeobacter violaceus PCC 8105 (AF132791)
0.02

Fig. 7

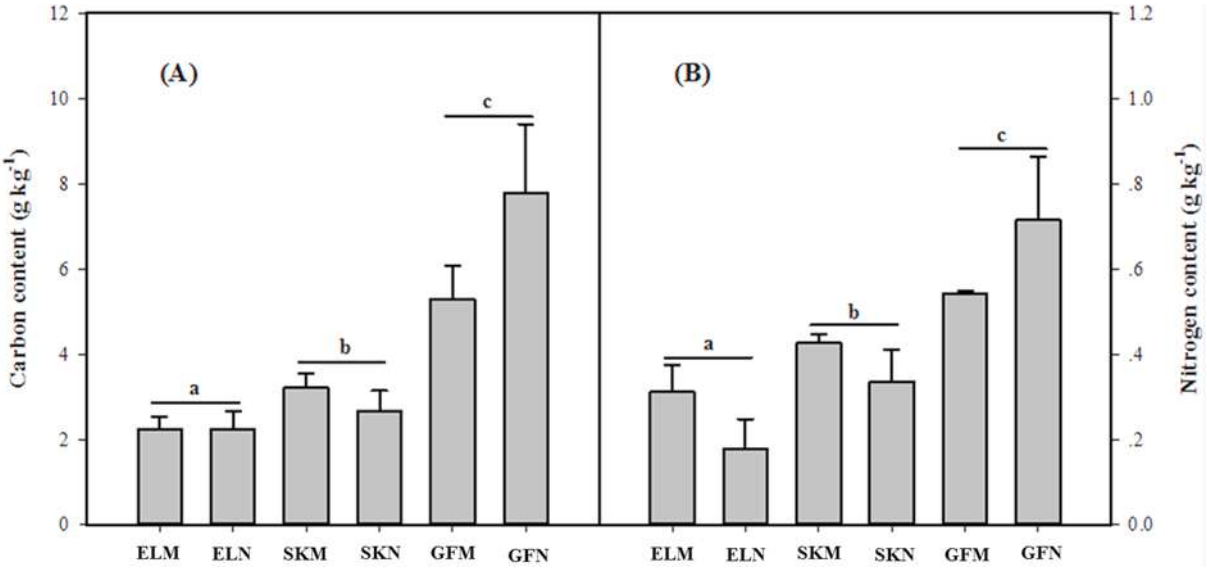
(A)
(B)
Carbon content (g kg-1)
Nitrogen content (g kg-1)
12
10
8
6
4
2
0
1.2
1.0
.8
.6
.4
.2
0.0
a
b
c
ELM
ELN
SKM
SKN
GFM
GFN

Fig. 8

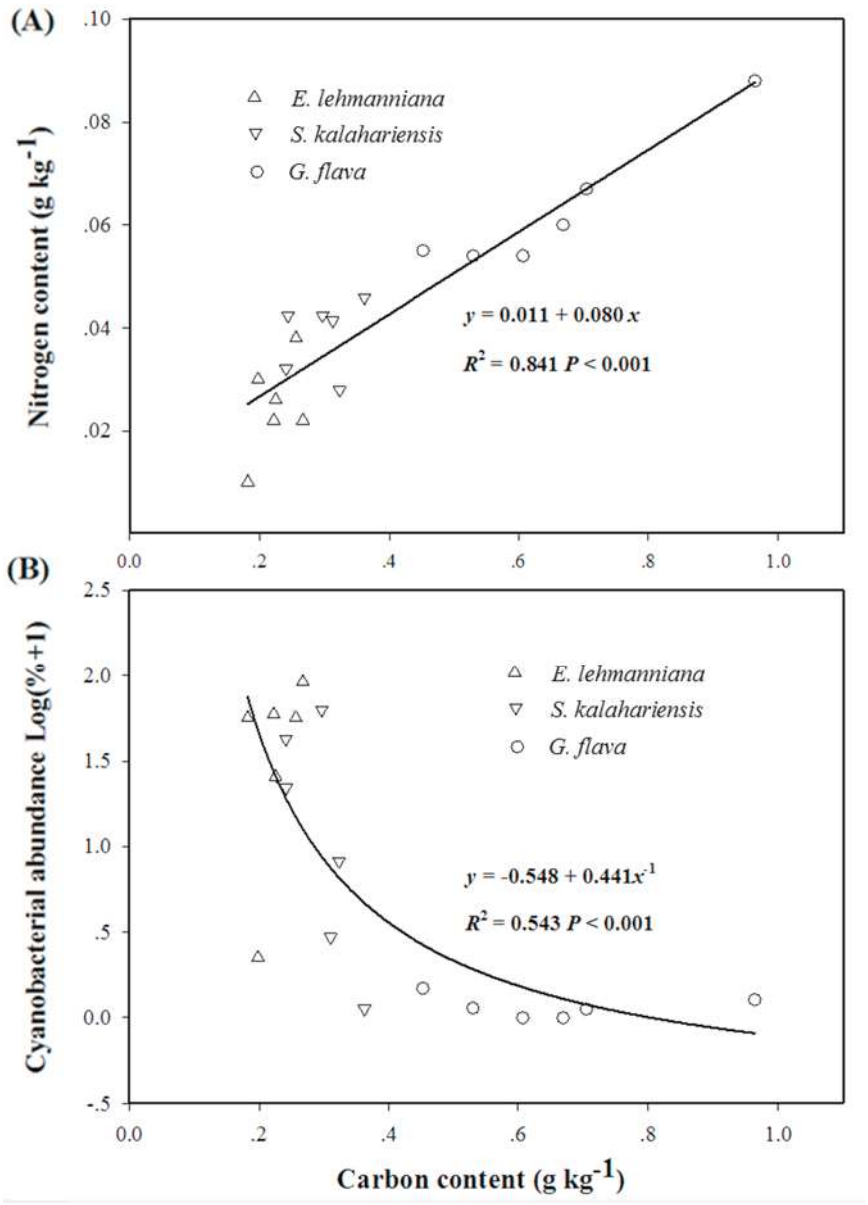
(A)
Nitrogen content (g kg-1)
.10
.08
.06
.04
.02
0.0
.2
.4
.6
.8
1.0
E. lehmanniana
S. kalahariensis
G. flava
y = 0.011 + 0.080 x
R2 = 0.841 P < 0.001
(B)
Cyanobacterial abundance Log(%+1)
2.5
2.0
1.5
1.0
.5
0.0
-.5
E. lehmanniana
S. kalahariensis
G. flava
y = -0.548 + 0.441x-1
R2 = 0.543 P < 0.001
Carbon content (g kg-1)

*Credit Author Statement

Authorship contribution statement

Shubin Lan: Manuscript conceptualization, data analysis, writing first draft and subsequent editing; **Andrew D. Thomas:** Fieldwork data collection, soil chemical analyses, data analysis, writing and editing; **Stephen Tooth:** Writing and editing; **Li Wu:** Writing and editing; **David R. Elliott:** Fieldwork data collection, DNA extraction and analysis, writing and editing.

Declaration of Competing Interest

There are no conflicts to declare.